Research Article DOI: 10.36959/771/577

The Effect of Light Intensity on Quercus robur L. Leaf Structure and Silicon Content

Olena Nedukha* 🗓

ha* iD

Department of Cell Biology and Anatomy, Institute of Botany of the National Academy of Sciences of Ukraine

Abstract

This study aims to explore the microstructure, arrangement, and silicon content of *Quercus robur* leaves grown in shaded and sunlit areas in the southern steppes of Ukraine. The study aimed to identify the similarities and differences in the ultrastructure and silicon content of oak leaf epidermis under varying natural lighting conditions. Electron scanning microscopy and laser confocal microscopy were used. Results indicated that shading alters the ultrastructure of the oak leaf epidermis and its silicon content. Silicon accumulation occurs primarily in the trichomes, stomata, and usual epidermal cells of the oak leaf. The phenotypic plasticity of the studied leaves was evident in reduced leaf size and area and increased trichomes, stomata density, and silicon in the epidermis of leaf trees grown in direct sunlight. This plasticity improves the leaves' ability to absorb and reflect light, allowing for normal growth and function even under direct sunlight. The various features of oak leaves can be employed for practical applications.

Keyword

English oak, Light intensity, Shading, Leaf micromorphology, Silicon

Introduction

Studying the structural and functional organization of Quercus robur leaves is crucial for botany and forestry in Ukraine, as it is a major species forming forests. The practical utilization of its leaves, bark, seeds, and acorns in phytochemistry and pharmacology adds significant value to this research from both fundamental and applied perspectives. Phenolic acid, terpenoids, and tannins derived from oak exhibit anti-inflammatory, anti-diabetic, and antitumor properties. These compounds hold significant promise as potential drug candidates in the fight against infectious diseases [1]. The conservation of oak forests in Ukraine is a growing concern, as climate change brings about more windfalls and droughts, with the added impact of atmospheric pollution. Such factors adversely affect the sustainability of oak forests [2]. Conserving the common oak is a crucial measure for preserving Europe's natural landscapes in all their beauty and diversity since this tree species provides wildlife with habitat and food, as well as contributing to good air quality. Additionally, oak stands minimize soil erosion by decreasing sediment run off and enriching the surrounding soil with nutrients [3]. Tree leaves are the first to detect environmental changes and respond appropriately. The outer cell walls of the leaf epidermis serve as a barrier and primary transport route for sunlight, CO₂, and water, while also acting as the interface between plant organs and the environment [4]. Epidermal walls are where silicon inclusions are synthesized [5] and are crucial in regulating sunlight absorption by the surface of the leaf. Retaining the curled leaves boosts light flux absorption and helps in the process of photosynthesis [6].

The functioning and structure of leaf epidermis rely on temperature, humidity, and UV intensity. The steppes of Ukraine experience temperatures ranging between +22 and +30 °C and an average annual rainfall of 400-600 mm. Trees growing in this area are adapted to severe drought. The impact of natural and human-caused disasters on oak forests has been extensively researched. However, there is a lack of understanding about important issues such as the phenotypic plasticity of the species and the regeneration of oak stands in the steppe zone of Ukraine. This knowledge serves as the foundation for the conservation of oak forests' biological diversity. We assume that the growth of oak trees in southern Ukraine, where conditions feature strong solar radiation and

*Corresponding author: Dr. Nedukha Olena, Department of Cell Biology and Anatomy, Institute of Botany of the National Academy of Sciences of Ukraine, 2 Tereschenkivska st., Kyiv, 01601, Ukraine

Accepted: November 13, 2024

Published online: November 15, 2024

Citation: Nedukha O (2024) The Effect of Light Intensity on *Quercus robur* L. Leaf Structure and Silicon Content. J Bot Res 7(1):184-197

Copyright: © 2024 Nedukha O. This is an open-access article distributed under the terms of the Creative Commons Attribution License, which permits unrestricted use, distribution, and reproduction in any medium, provided the original author and source are credited.



limited water availability, may be attributable to specific traits of leaf epidermal structure withstanding the region's hot climate. To investigate, our study aimed to examine the leaf microstructure, arrangement, and silicon content of *Quercus robur* L. leaves grown both in shade and under direct sunlight in the southern steppes of Ukraine.

Material and Methods

Region and plant material

Our study focused on the leaves of the common oak, Quercus robur L. (Fagaceae), which grows in the steppe zone of the Dnepropetrovsk region of Ukraine (48°27′58"N, 35°01'31"E, 139 m above sea level). Oak leaves were collected on June 22, 2022, for the study. The sampling site of Q. robur has the following habitat characteristics: 1: A forest of southern ravine-oak variety grows on the edge of a stand near the village of Bashmachka in the Solonyansky district of the Dnepropetrovsk region, on the right bank of the Dnipro river in Ukraine. At site 2, on the top of a ravine, two oaks (Nos. 1 and 2) grow, while site 1 hosts oaks (Nos. 3 and 4). Refer to Table 1 for more information. Specifically, Oak No. 1 grows at the forest edge, Oak No. 2 grows in dense forest, and Oak Nos. 3 and 4 grow alone. In late June, Ukraine's Dnepropetrovsk Region experienced hot weather caused by a powerful anticyclone. The average daily air temperature in June was significantly higher than normal. For 3-6 days, the maximum air temperature surpassed 30 °C and reached 33-37 °C on the hottest days. The average 10-day air temperature was 1.2-3.8 °C above the multiyear average and ranged from +20.6-23.0 °C. There was a precipitation deficit for most days during the ten-day period. High air temperatures and a significant lack of precipitation led to intense moisture loss, particularly in the upper soil layer. The region experienced an ongoing crop drought (source: https://www.apk-inform.com).

On the day of collection, the weather was sunny. The amount of light on the leaf surface differed between oak trees #1, #2, #3, and #4. PPFD (photosynthetic photon flux density) levels on the adaxial surface of oak #1 leaves were 900 µmol·m⁻²·s⁻¹; for oak #2, it was 50 µmol·m⁻²·s⁻¹. The LI-250 light meter (USA, LI-COR) was used to measure the PPFD. Light intensity was measured on the upper surface of the lowermost tier of leaf plates for cytological analyses. 15-20 leaves were collected from each tree's branches, and their length and breadth were measured. To carry out these analyses, we used the center portion of every other (upper)

lobe from five leaves of each type (Figure 1).

The leaf area was determined following the procedure outlined by Pandey and Singh [7]. Each leaf was placed on a sheet of graph paper with millimeter markings, and the outline was traced. The sheet area was then measured using a meter. A section of graph paper, equivalent to the leaf's outline, was cut using a paper knife and weighed on an electronic scale. Similarly, one square centimeter of the same graph paper was cut and weighed. Leaves from the same sample were measured multiple times. The area of the leaf was calculated using the non-destructive method with the following equation: Leaf area can be determined using the following formula: Area (square cm) = weight of paper within the outline (g)/weight of paper per cm² (g/cm²). To describe the mophology of the leaves, we used the features used by botanists in the study of oak systematics [8].

Scanning electron microscopy

The middle portion of each second upper lobe of the leaf plate was fixed in a solution consisting of 2% paraformaldehyde and 1% glutaraldehyde (1:1, vol.) in 0.5 M phosphate buffer (pH 7.2) for 3 hours at +4 °C (in a thermos). After bringing them to the laboratory, wash the samples with the same buffer and dehydrate them in a series of alcohols (70%, 80%, and 100% ethanol; twice every 30 minutes) as per Talbot and White's [9] protocol. After dehydrating the samples, they were mounted on aluminum tables, coated with carbon and gold, and analyzed using a JSM 6060 LA scanning electron microscope at 30 kV. Cell size was determined by measuring 30-40 usual epidermal cells, 30-35 stomata, and 20-25 trichomes in three samples from each of the five leaves. All measured variables were then analyzed for variance using the Origin 6.1 program.

Laser confocal microscopy

Samples for laser confocal microscopy were prepared following Dabney, et al., [10] procedure. We exposed sections from the middle of the second (upper) leaf blade of the leaf plate of five leaves from each oak tree (10 \times 20 mm) to +220 $^{\circ}$ C for three hours until the samples turned gray. The study analyzed the presence of silicon in leaf samples employing an LSM5 laser scanning confocal microscope (Zeiss, Germany) with excitation and emission wavelengths of 480 nm and 530 nm, respectively. The study considered five leaves from each tree. The silicon fluorescence intensity was then evaluated using the Pascal program on the LSM5.

Table 1: Basic parameters of the sampled Q. robur trees and their habitat (Dnipropetrovsk Region near village of Bashmachka).

Oak tree number	Approximate oak age, years	Light intensity on sampling day, µmol·m ⁻² ·s ⁻¹	Oak habitat	Shadiness at the level of lower oak branches, %
No. 1	~130-150	900*	Single trees on the forest edge dese forest	40.0
No. 2	~50	50	Dense forest	96.6
No. 3	~80	1500	Single trees in the upper reaches of a gully	0.0
No. 4	~80	1500	Single trees in the upper part of a gully	0.0

^{*}Light intensity was measured on the upper surface of leaf blades from the lowest tier of branches. These leaves were used for cytological studies

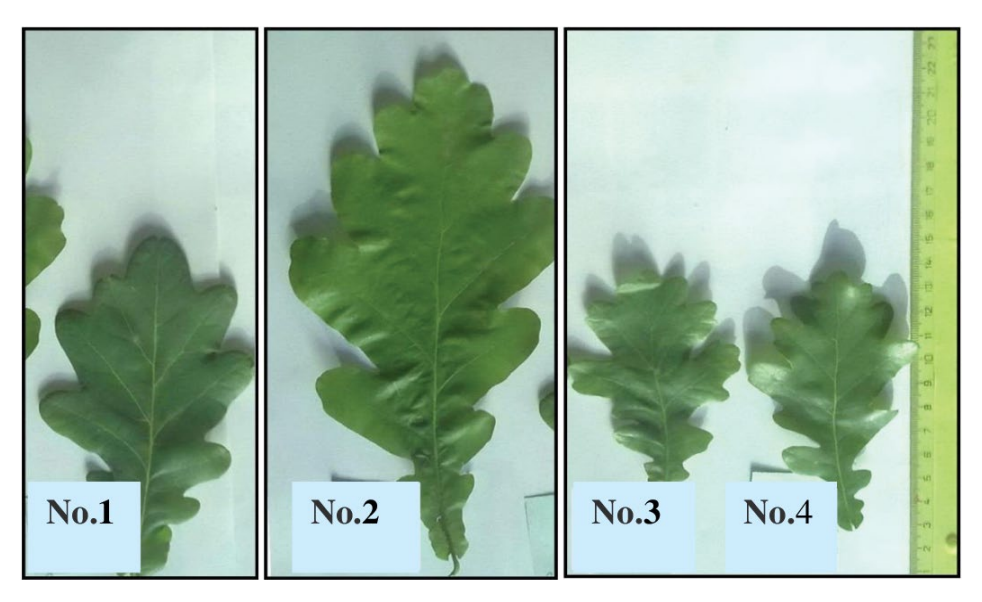


Figure 1: Common view of leaf blades from four *Quercus robur* trees growing in Dnipropetrovsk Region, Ukraine. Trees No. 1 and No.2 grow among other trees in the shade; trees No. 3 and No. 4 grow separately from other trees without shade.

Table 2: Morphological parameters of leaves of *Q. robur* growing in the southern steppes of Ukraine, Dnipropetrovsk Region. 'a' notes significant differences in parameters between tree No. 1 (shaded) and No. 3 (unshaded) ($P \le 0.05$), while 'b' notes significant differences within the parameters of a single tree. 2 (Shaded trees) from tree No. 3 (without shading) ($P \le 0.05$). "c" indicates significant differences in parameters for trees No. 1 (shaded) and No. 4 (unshaded) ($P \le 0.05$), while "d" indicates significant differences in parameters for trees No. 2 (shaded) and No. 4 (unshaded) ($P \le 0.05$).

Parameter Leaf size, mm	Oak tree number				
	Tree No. 1	Tree No. 2	Tree No. 3	Tree No. 4	
Long axis	105 ± 9.1	130 ± 12.1	75 ± 7.1 ^{a,b}	78 ± 5.7 ^{c,d}	
Short axis (in the 2 nd lobe)	42 ± 5.7	57 ± 3.7	33 ± 5.1 ^{a,b}	32 ± 3.9 ^{c,d}	
Leaf area*, mm²	4665 ± 133	6057 ± 141	3188 ± 153 ^{a,b}	2729 ± 131 ^{c,d}	

^{*}Leaf area was measured by the protocol of Pandey and Singh (2011)

Statistics

Statistical differences among mean values were determined using the Student's t-test with a significance level of P < 0.05. Significant differences were observed across all measurements. Origin 6.1 software was employed for data analysis. Each experiment was conducted three times. We measure leaf size, trichome and epidermal cell size, stomata density, and the microstructure of the leaf surface, or the cytochemical study of the fluorescence of silicon inclusions. For cytological research, we chose 20-22 medium-sized leaves from the lower branches of every oak tree. Ten leaves from each variant were chosen to measure linear dimensions, and five leaves were selected for studying the microstructure of the leaf epidermis and five leaves for conducting cytochemical research on silicon. The average size of the leaf blades for the four oak trees is shown in Table 2. The length of the blade, from the apex to the petiole, and width at the level of the second upper lobe are the first and second values, respectively. The mean value comparison between leaves was done through ANOVA. Origin 6.1 programs performed the analysis of variance for all measured variables.

Results

Micromorphology of Quercus robur L. leaves

The surface structure of the leaves of four oak trees was studied. Trees No. 1 and No. 2 grew in the shade in a group of trees on the edge of the forest near the village of Bashmachka in the Dnipropetrovsk Region. While Trees No. 3 and No. 4 grew individually on ravine tops in direct sunlight without shade (see Table 1 for the basic parameters of the samples), Leaves from four selected common oak Q. robur trees, regardless of age or growth location, display comparable leaf blade characteristics: the leaves have a short petiole, are hypostomatic (stomata present only on the lower surface of the blade), are elongated-obovate in shape (as shown in Figure 1, are narrowed downwards, and are pinnately lobed. The leaf blades are rounded and blunt, with shallow notches between them. Some variations in leaf size, area, and ultrastructure were observed in the leaf epidermis. Table 2 displays the average leaf blade size of the four trees studied.

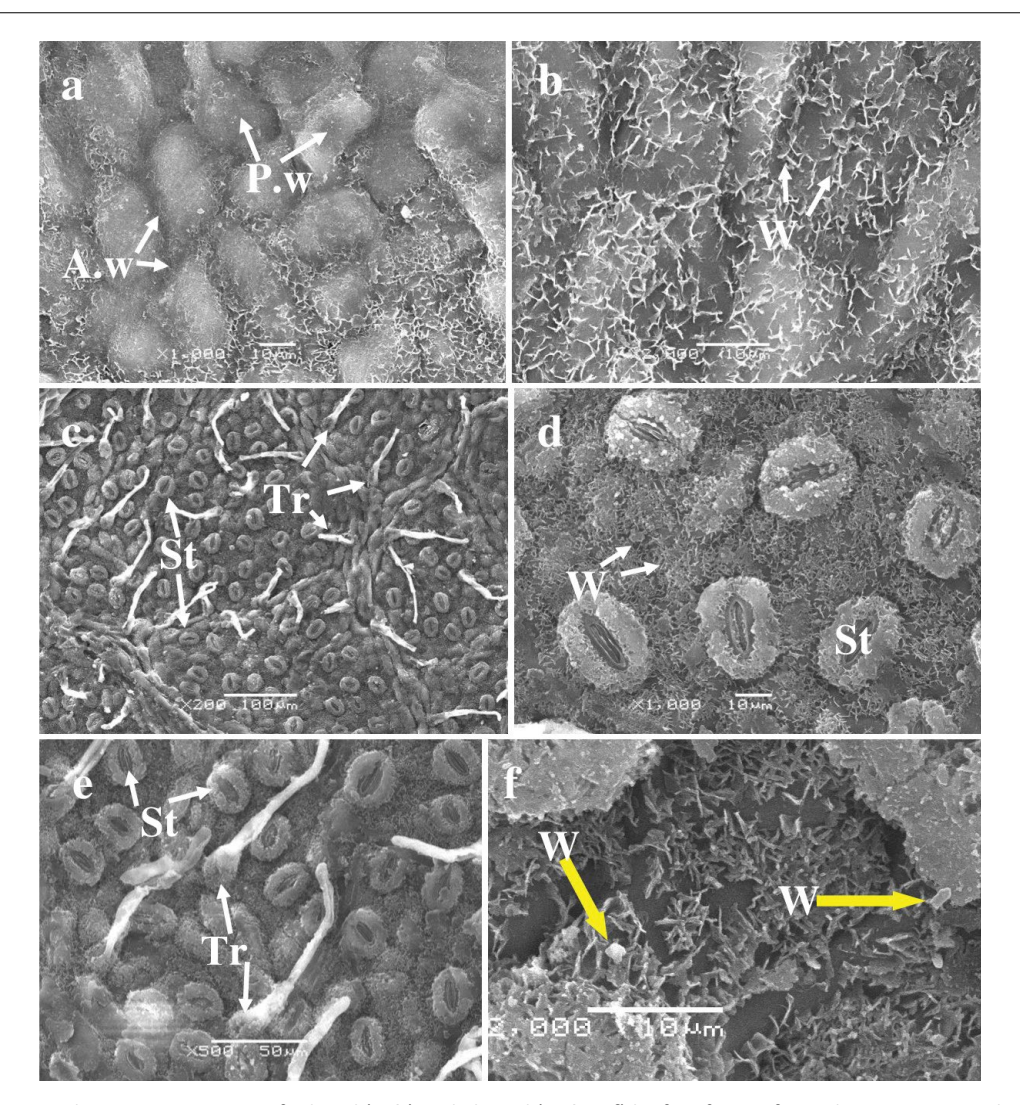


Figure 2: Scanning electron microscopy of adaxial (**a**, **b**) and abaxial (**c**, **d**, **e**, **f**) leaf surfaces of *Q. robur* tree No. 1, which is growing in the shaded forest of Dnipropetrovsk Region, Ukraine. The yellow arrows indicate the location of wax crystals. Abbreviations used include A.w: Anticlinal Wall; P.w: Periclinal Wall; St: Stomata; Tr: Trichrome; and W: Wax.

Scanning electron microscopy

Leaves of tree No. 1

Adaxial surface: The oak leaves under study exhibited an irregular upper epidermal surface. The periclinal walls of epidermal cells protruded above the surface. Such walls form spherical or ovoid bulges, around which anticlinal walls produce depressions that cover needle-like and lamellar waxy structures, varying in size from 1 to 4 μm (Figure 2a and Figure 2b; Table 3). Stomata and trichomes were absent from the upper epidermis. The periclinal wall protrusions exhibit a partially smooth surface, sometimes coated with wax structures, reminiscent of the appearance of the anticlinal recessed walls.

The abaxial epidermis: The lower epidermis of oak leaves contains stomata and trichomes, which originate from the lower epidermal cells and the cells of the protruding veins (Figure 2c, Figure 2d, Figure 2e, and Figure 2f).

The lower epidermal cells are covered by a layer of lamellar crystalline structures, making it difficult to see and measure their boundaries and sizes. Table 3 provides details

on the density of stomata and trichomes, as well as the average size of stomatal cells and trichomes. The stomata are oval-elongated; with guard cells covered by thin crystalline structures approximately 2 μ m in size. While the stomatal gap is free of crystalline structures. Trichomes on the leaf surface are simple, slightly raised, and unbranched, with a drop-shaped base, rounded-plate-shaped main parts, and pointed apices. The base of the trichomes is covered by small, stick-shaped crystalline structures, sometimes accompanied by larger, crystal-like structures (Figure 2f).

Leaves of tree No. 2

The adaxial surface of leaves from tree number 2 is distinct, with clearly defined epidermal cell contours and an absence of stomata and trichomes (Figure 3a and Figure 3b). Anticlinal walls protrude above the epidermal surface, forming a tall fence around each cell. The cells on the upper leaf surface are small and have a similar shape to those on tree number 1 (Table 3). The periclinal walls are depressed, and both the anticlinal and periclinal cells are uniformly covered with crystalline structures measuring 1 to 3 μm in size.

Table 3: The structural parameters of *Q. robur* leave of trees. ^adenotes significant differences in the parameters in tree No. 1 (shading) and No. 3 (without shading) ($P \le 0.05$); ^bdenotes significant differences in the parameters in the tree No. 2 (shading) and No. 3 (without shading) ($P \le 0.05$); ^cdenotes significant differences in the parameters in the tree No. 1 (shading) and No.4 (without shading) ($P \le 0.05$); ^ddenotes significant differences in the parameters in the tree Nr 2 (shading) and No.4 (without shading) ($P \le 0.05$).

Parameter	Oak tree number				
	Tree No. 1	Tree No. 2	Tree No. 3	Tree No. 4	
Adaxial epidermis					
Size of pavement cell, μm					
Long axis	23 ± 1.3	21 ± 1.3	25 ± 1.2	26 ± 1.2	
Short axis	20 ± 1.2	18 ± 1.1	24 ± 1.7	23 ± 1.3	
Abaxial epidermis					
Size of pavement cell, μm	Not determined*	Not determined*	Not determined*	Not determined*	
Stomata:					
Density, number per mm² area	350 ± 21	380 ± 27	531 ± 37 ^{a,b}	429 ± 47 ^{c,d}	
Long axis of guard cell , μm	29 ± 1.2	23 ± 1.7	28 ± 1.3	30 ± 1.1	
Short axis of guard cell, μm	11 ± 0.4	10 ± 0.4	10 ± 0.1	12 ± 0.7	
Trichome:					
Density, number per mm² area	78 ± 8.9	71 ± 7.0	87 ± 7.3 ^{a,b}	86 ± 7.9 ^{c,d}	
Long axis, μm	98 ± 7.1	82 ± 7.3	72 ± 8.9	76 ± 9.5	
Short axis in the base, µm	20 ± 1.5	13.6 ± 1.3	21 ± 1.2	20 ± 1.5	
Short axis in the middle, µm	8.3 ± 0.1	7.3 ± 0.1	7.3 ± 0.7	8.0 ± 0.3	

^{*}The surface of the pavement cells of the lower epidermis is covered with a ontinuous layer of lamellar rystalline structures, so the boundaries of the pavement cells of the lower epidermis are not visible and their sizes are not determined.

On the abaxial surface, the lower epidermal cells are concealed by a continuous layer of lamellar crystalline structures, while stomata and trichomes are present (Figures 3c, Figure 3d, Figure 3e, and Figure 3f). The size of the main cells cannot be determined, as seen in sample 1. Additionally, fine crystalline structures that measure approximately 2 μ m enclose the stomatal guard cells. The mean density of trichomes is 71 \pm 7.0 per square millimeter of surface area. Trichomes extend from the cells of protruding veins and are positioned above the usual cells. They are simple, unbranched, and slightly raised, with a distal base that is drop-shaped and a middle part that is rod-shaped and pointed at the apex. The trichome base is covered with small, crystalline, rod-shaped structures. The average sizes of stomatal guard cells and trichomes can be found in Table 3.

Leaves of tree No. 3

Adaxial Surface: An analysis of the leaf ultrastructure of Tree #3 revealed similar characteristics to those of Tree #1. The periclinal walls of the epidermal cells protruded above the surface, creating spherical or ovoid bulges where the anticlinal walls formed depressions. These depressions were covered in needle-like and lamellar waxy structures ranging in size from 1 to 4 μm (Figure 4a and Figure 4b). Stomata and trichomes were absent on the upper epidermis. The surface of the periclinal wall protrusions is partially smooth, sometimes covered with waxy structures, similar to the surface of the anticlinal recessed walls. The cell sizes on the adaxial surface are listed in Table 3.

Abaxial Surface: On the lower surface of the specimen, the

abaxial surface, stomata and trichomes are visible (Figure 4c, Figure 4d, Figure 4e, and Figure 4f). Trichomes emerge from the pavement cells and from the cells of protruding veins. The stomata are slightly elongated and oval-shaped. The density and size of stomata are listed in Table 3. Stomatal guard cells are covered with thin crystalline structures measuring about 2 μm , while the stomatal gap is free of such structures. The average size of the stomatal gap measures $18\pm0.6\times5\pm0.2$ μm . The stomatal surrounding pavement cell surface is also coated in a continuous layer of lamellar crystalline structures, which renders the boundaries of the ordinary cells of the lower epidermis indiscernible.

The trichomes are situated above the primary epidermal cells, tilted slightly upward, and occasionally above the veins. The apex base of the trichomes assumes a drop shape; the main part is plate-shaped and crystalline. The lower epidermal usual cells surrounding the stomata and the cells beneath the trichomes are covered by a continuous layer of lamellar crystalline structures. As a result, the borders of the usual cells surrounding the stomata are not visible, which is similar to the structure of the epidermal cells in leaves of trees No. 1 and No. 2. The trichome base is also covered with small, rod-shaped crystalline structures and occasionally has larger crystal-like structures as well (Figure 4f). The average sizes of stomatal closure cells and trichomes are provided in Table 3.

Leaves of tree No. 4

Adaxial Surface: The ultrastructure analysis of the adaxial leaf surface of Tree No. 4 revealed the absence of trichomes and stomata. The epidermis surface was composed of typical

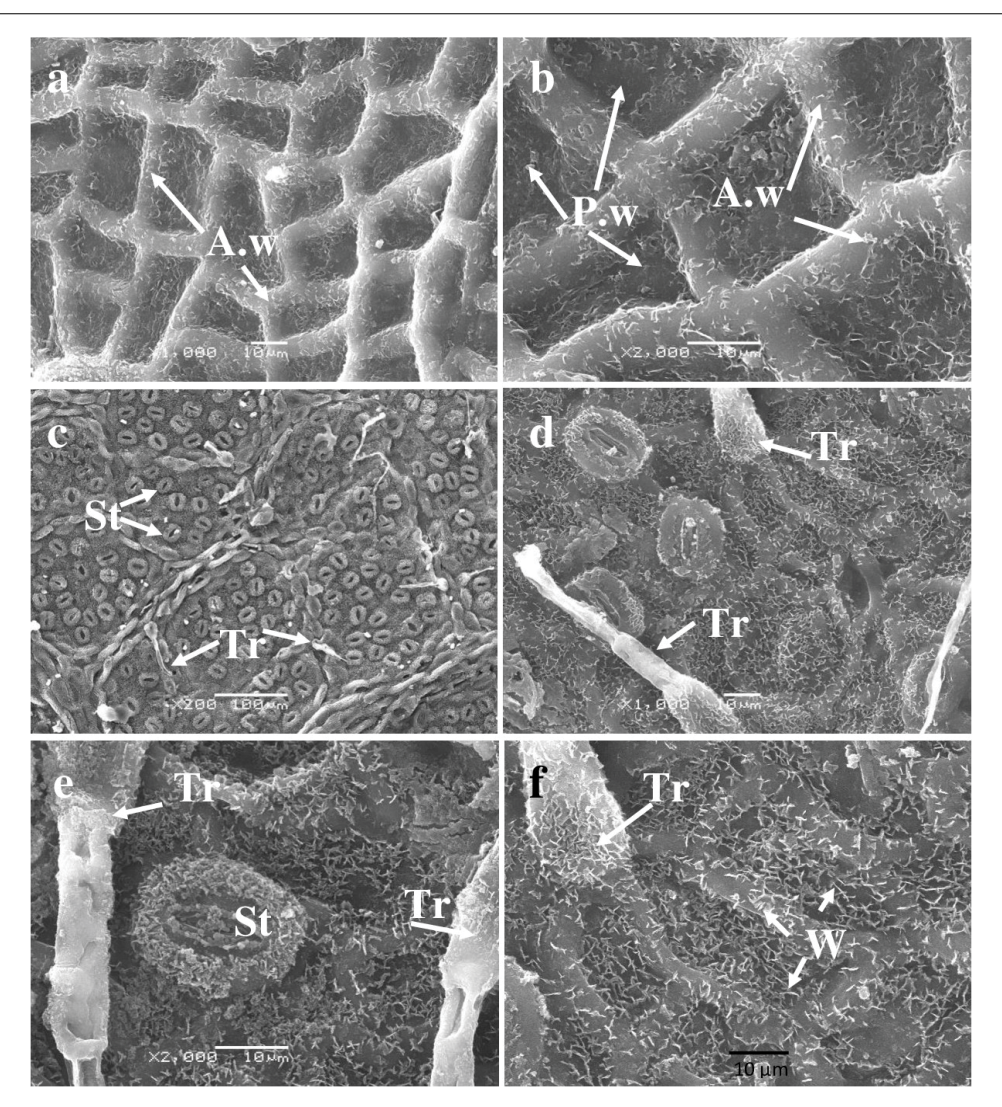


Figure 3: Scanning electron microscopy images of adaxial (a, b) and abaxial (c, d, e, f) surfaces leaves from *Q. robur* tree No. 2, growing in the shaded forest of Dnipropetrovsk Region in Ukraine. Abbreviation: A.w: Anticlinal Wall; P.w: Periclinal Wall; St: Stomata; Tr: Trichrome; W: Wax.

epidermal cells, with periclinal walls projecting above the surface and anticlinal walls recessed (Figures 5a and Figure 5b).

The spherical or ovoid bulges protruding from the periclinal walls of the epidermal cells resulted in depressions formed by the anticlinal walls. These depressions were covered in needle-like and lamellar wax structures of varying sizes, ranging from one to four μm . Both the anticlinal walls and parts of the periclinal walls were covered in waxy structures. Stomata and trichomes were not present on the upper epidermis. The periclinal wall projections of most cells have a smooth surface, although some periclinal walls and the surface of the anticlinal recessed walls are occasionally covered with waxy structures. Table 3 presents the cell size on the adaxial surface.

Abaxial Surface: The leaves of Oak No.4 exhibit stomata and trichomes (Figures 5c, Figure 5d, Figure 5e, and Figure 5f) that originate from the main epidermal cells and the vein cells. The stomatal guard cells are coated with needle-like waxy structures that measure approximately 2 μ m. The

stomatal gap lacks crystalline structures with an average size of 17 \pm 1.3 \times 5 \pm 0.2 μm . The lower epidermal cell surface that encircles the stomata features a constant waxy layer in diverse forms - needle-like, lamellar, and crystalline. Trichomes sit atop the main epidermal cells, being slightly lifted and occasionally positioned over the veins. They are simple, raised, and unbranched with an elongated or oval base and a rod-shaped head. The trichome base is encompassed with needle-like waxy structures. The boundaries of the usual cells in the lower epidermis are rendered invisible by the continuous layer of lamellar crystalline structures that cover the surface of the epidermal cells surrounding the stomata, a feature consistent with previous specimens. The average size of stomata cells and trichomes can be found in Table 3.

Evaluation of laser confocal microscopy results of silicon inclusions

Leaves of tree No. 1

Our study shows the bright green fluorescence of silicon inclusions in the epidermal cells of oak tree No. 1 leaves (Figure

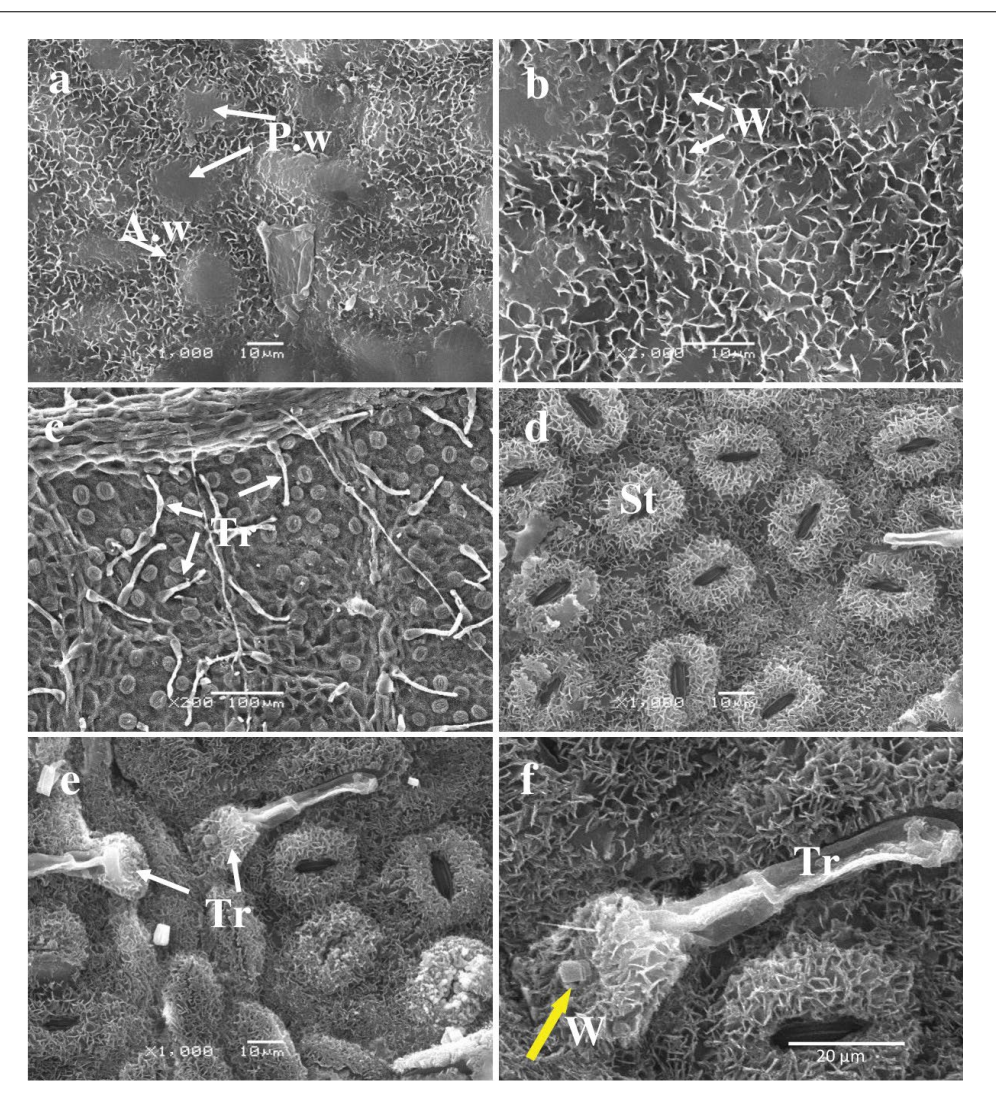


Figure 4: Scanning electron microscopy of adaxial (**a**, **b**) and abaxial (**c**, **d**, **e**, **f**) leaf surfaces of *Q. robur* tree No. 3 in the shaded forest of Dnipropetrovsk Region, Ukraine. A yellow arrow indicates wax crystal (fig. **f**). Abbreviation used: A.w: Anticlinal Wall; P.w: Periclinal Wall; St: Stomata; Tr: Trichrome; W: Wax.

Table 4: The intensity profile of silicon inclusions (in relative units) in cell walls of the leaf epidermis of *Q. robur* shaded trees (No. 1 and No. 2) and unshaded trees (No. 3 and No. 4); data are means \pm SD of three replicates; 30-35 cells of each type in the epidermis were used in each replicate. ^asignifies notable variations in the factors of tree No. 1 (with shading) from tree No. 3 (without shading) ($P \le 0.05$); ^bindicates substantial divergences in the variables of tree No. 2 (with shading) from tree No. 3 (without shading) ($P \le 0.05$); ^cshows noteworthy differences in the parameters of tree No. 1 (with shading) from tree No. 4 (without shading) ($P \le 0.05$); ^ddenotes noteworthy disparities in the parameters of tree No. 2 (with shading) from tree No. 4 (without shading) ($P \le 0.05$);

Parameter	The intensity profile of silicon fluorescence in the leaf of oak four trees, relative units				
	Tree No.1	Tree No. 2	Tree No. 3	Tree No. 4	
Adaxial epidermis					
Anticlinal wall of pavement cells	120 ± 13.0	105 ± 11.0	140 ± 12 ^b	145 ± 13 ^{c,d}	
Periclinal wall of pavement cells	70 ± 5.3	55 ± 4.3	124 ± 11 ^{a,b}	115 ± 12 ^{c,d}	
Trichome	Absent	Absent	Absent	Absent	
Stomata	Absent	Absent	Absent	Absent	
Abaxial epidermis					
Anticlinal wall of pavement cells	75 ± 8.8	80 ± 9.3	100 ± 9.7 ^{a,b}	120 ± 11 ^{c,d}	
Periclinal wall of pavement cells	70 ± 5.3	23 ± 1.7	82 ± 5.4 ^{a,b}	95 ± 7.7 ^{c,d}	
Trichome	156 ± 11	121 ± 12.0	180 ± 15 ^{a,b}	185 ± 12 ^{c,d}	
Stomata	71 ± 5.4	65 ± 7.1	125 ± 12 ^{a,b}	128 ± 11 ^{c,d}	

6a, Figure 6b, Figure 6c, and Figure 6d). The fluorescence of the silicon was detected in the anticlinal and periclinal walls of the adaxial epidermis (Figure 6a).

The silicon inclusions were densely arranged in the anticlinal walls, forming nearly continuous layers. Individual silicon inclusions are visible in the periclinal walls. Silicon fluorescence is noticeable in the walls of epidermal cells, guard cells of stomata, and at the base of trichomes in the lower epidermis. The silicon had a single, individual inclusion in its form (Figure 6b). The intensity of the silicon fluorescence profile varied among the studied cells and depended on the leaf surface and cell type (Table 4; Figure 6c, Figure 6c', Figure 6d, and Figure 6d'). The silicon intensity varied between the anticlinal and periclinal walls of epidermal cells on the adaxial surface. The intensity in anticlinal walls was 120 \pm 13 relative units, while in periclinal walls, it was significantly lower, quantifying to 70 ± 5.3 relative units. Furthermore, the intensity of silicon in the anticlinal walls of ordinary cells of the lower epidermis was 75 ± 8.8 relative units. In contrast, in the periclinal walls of those cells, it was 70 ± 5.3 , and in trichomes and the closing cells of stomata, it was 156 ± 11 and 71 ± 5.4 relative units, respectively. The silicon inclusions are most densely concentrated in the anticlinal walls of the adaxial epidermis and in the trichomes of the abaxial epidermis.

Leaves of tree No. 2

The analysis showed green silicon fluorescence in the cell walls of epidermal cells in both the upper and lower epidermis, as well as in stomata and at the base of trichomes in Q. robur leaves of tree No. 2, which were grown in shade (Figures 6e and Figure 6f). Additionally, silicon fluorescence was detected in the anticlinal and periclinal walls of the main epidermal cells of the adaxial epidermis (Figure 6g). The relative units of the fluorescence intensity were 105 \pm 11.0 and 55 \pm 4.3, respectively. Silicon fluorescence was also found in the guard cells of stomata, at the base of trichomes, and in the anticlinal and periclinal walls of epidermal cells in the abaxial epidermis, consistent with the previous sample. The intensity of the silicon profile varied depending on the leaf surface and cell type, as shown in Table 4 and Figures 6g, Figure 6g', Figure 6h, and Figure 6h'. Silicon levels were 80 \pm 9.3 in anticlinal walls, 23 \pm 1.7 in periclinal walls, 121 ± 12 in trichomes, and 65 ± 7.1 in stomata,

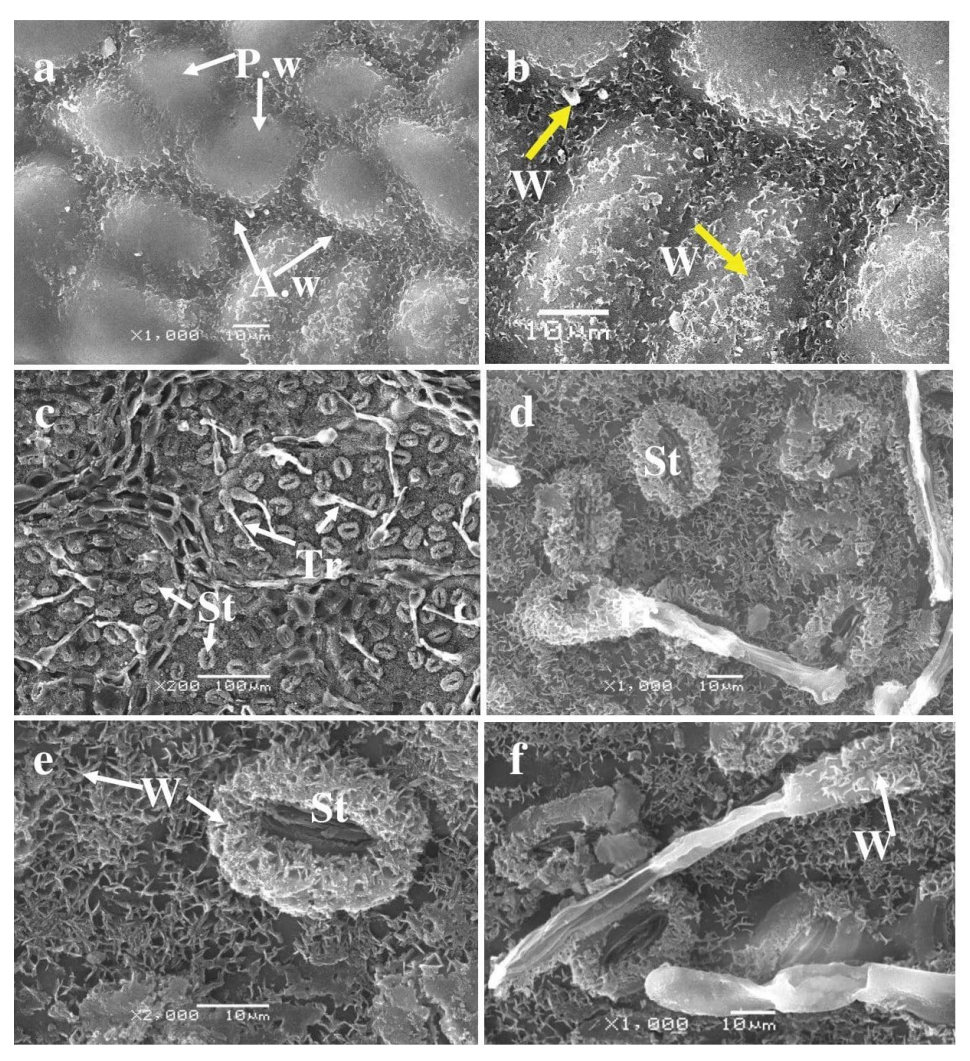


Figure 5: Scanning electron microscopy images of the adaxial (**a**, **b**) and abaxial (**c**, **d**, **e**, **f**) leaf surfaces of *Q. robur* tree No. 4, which was grown in the shaded forest of Dnipropetrovsk Region, Ukraine. The following abbreviations are used: Figure b highlights the presence of wax crystals, as indicated by yellow arrows. A.w: Anticlinal Wall; P.w: Periclinal Wall; St: Stomata; Tr: Trichrome; and W: Wax.

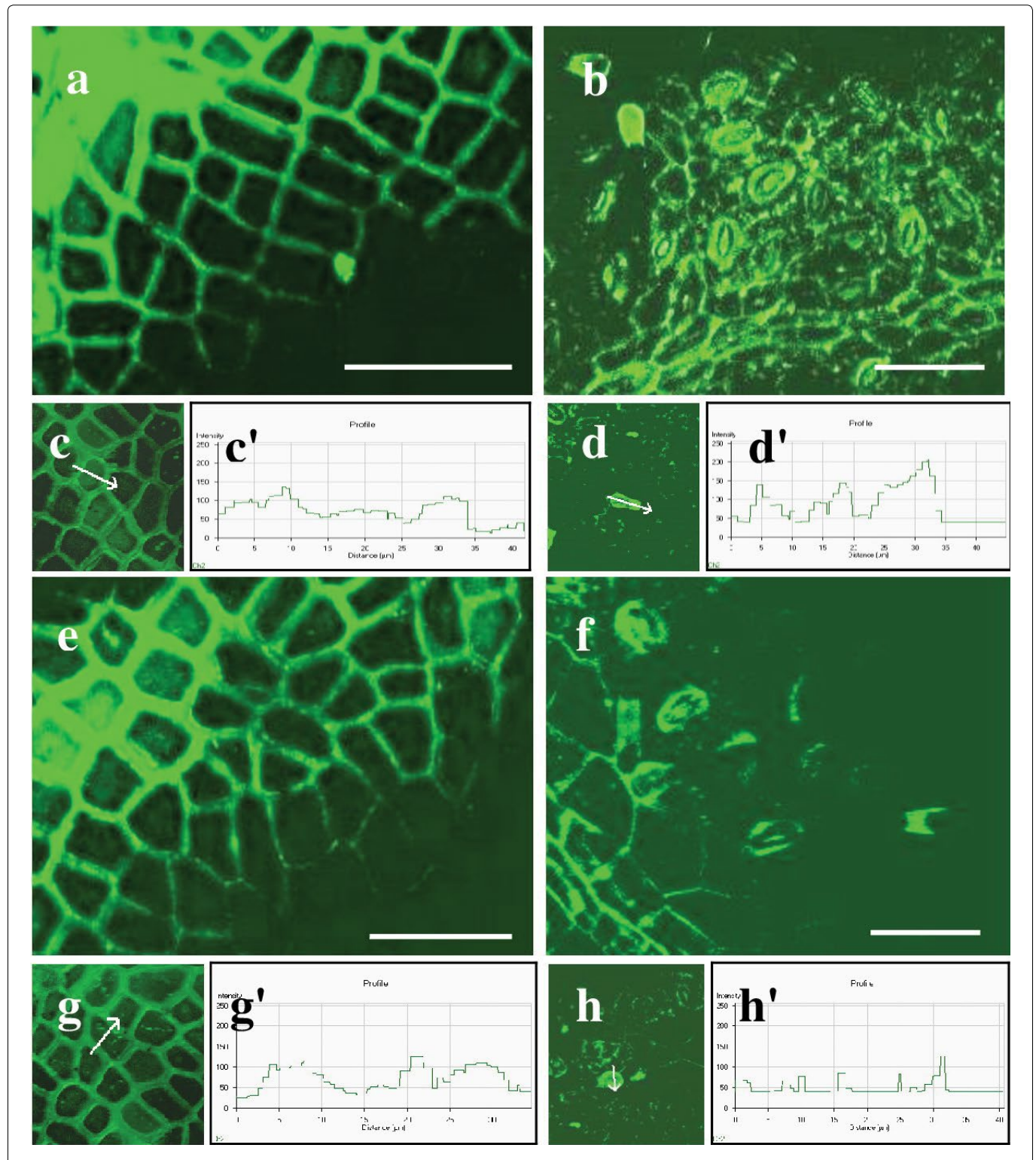


Figure 6: Fluorescence of silicon inclusions visualized with confocal laser scanning microscopy for the adaxial (a, e) and abaxial (b, f) surface of leaves in two *Q. robur* trees (a-d - No. 1 and e-h - No. 2). Silicon has green fluorescence. Figures c', d', g', and h': histograms of the intensity profile of silicon (green line). Ordinate of the histograms indicates the intensity profile of green line, while the abscissa indicates the distance (μm) scanned in c, d, g and h; with the this white line illustrating this distance on c, d, g and h. Bars = 50 μm.

all reported in relative units. In summary, the periclinal walls of the primary cells on the upper and lower surfaces, including the walls of stomata, have low profile intensity.

Leaves of tree No. 3

A cytochemical analysis of silicon in Q. robur leaves was

conducted on tree No. 3, which grew in direct sunlight without shade. The results revealed green fluorescence of silicon in the walls of upper epidermal cells, trichomes, stomata, and conducting bundle cells (Figures 7a, Figure 7b, Figure 7g, and Figure 7h).

Silicon fluorescence was also observed in various parts

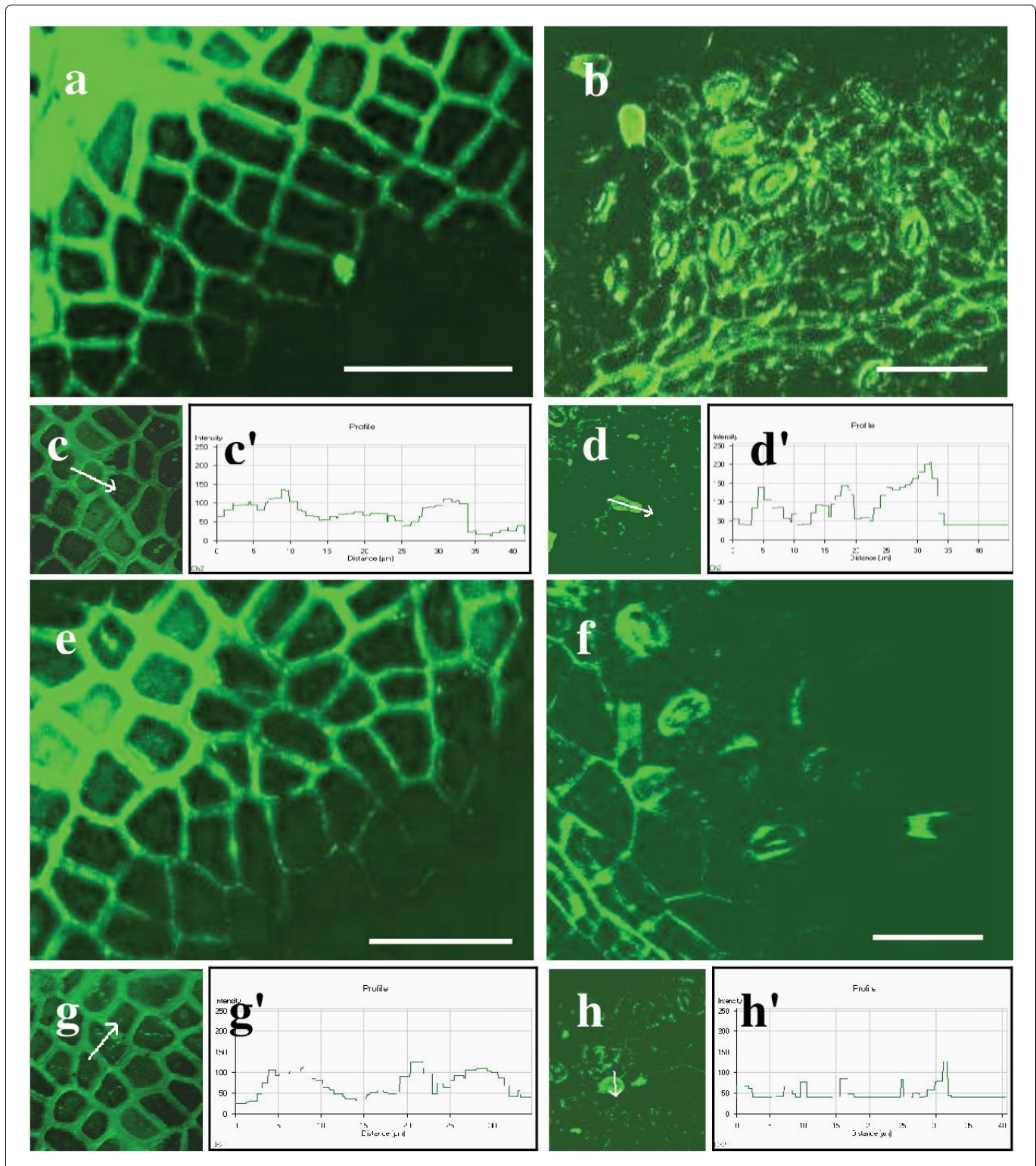


Figure 7: Fluorescence of silicon inclusions visualized with confocal laser scanning microscopy for the adaxial (a, e) and abaxial (b, f) surface of leaves in two *Q. robur* trees (a-d - No. 1 and e-h - No. 2). Silicon has green fluorescence. Figures c', d', g', and h': histograms of the intensity profile of silicon (green line). Ordinate of the histograms indicates the intensity profile of green line, while the abscissa indicates the distance (μm) scanned in c, d, g and h; with the this white line illustrating this distance on c, d, g and h. Bars = 50 μm.

of the leaf, including the abaxial epidermis, guard cells of stomata, trichome base, and epidermal cell walls. The intensity of the silicon profile varied depending on the leaf surface and cell type, measured in relative units. The highest intensity was found in the anticlinal and periclinal walls of the upper epidermis, with values of 140 ± 12 and 124 ± 11 relative

units, respectively. Similarly, the intensity of the profile was high in the anticlinal walls of the lower epidermis, at the base of trichomes and stomata guard cells, with values of 100 ± 9.7 , 180 ± 15 , and 125 ± 12 relative units, respectively. However, the periclinal walls of lower epidermal cells showed a lower profile intensity of 80 ± 5.4 relative units (See Table 4; Figures

7c, Figure 7c', Figure 7d, and Figure 7d').

Leaves of tree No. 4

The cytochemical analysis revealed green fluorescence for silicon within the walls of ordinary epidermal cells, trichomes, stomata, and conducting bundle cells. In the adaxial epidermis, silicon fluorescence was detected in the anticlinal and periclinal walls of the upper epidermal cells, similar to the previous sample (Figures 7e and Figure 7f). Silicon fluorescence was also detected in the anticlinal and periclinal walls of the abaxial epidermal cells, guard cells of stomata, and trichome bases. The intensity of the silicon profile varied based on the leaf surface and cell type, as indicated in Table 4 and Figures 7g, Figure 7g', Figure 7h, and Figure 7h'. The highest silicon profile intensity was in the anticlinal and periclinal walls of the upper epidermis, with relative units of 145 ± 13 and 115 ± 12, respectively. Additionally, significant profile intensity was found in the anticlinal walls of the lower epidermis, trichomes, and stomatal guard cells, with values of 120 ± 11 , 185 ± 12 , and 128 ± 11 relative units, respectively. Conversely, the periclinal walls of ordinary cells in the lower epidermis demonstrated lower profile intensities, measuring just 95 ± 7.7 relative units.

Discussion

The examination of leaf surface ultrastructure of four Q. robur trees in Ukraine's Dnipropetrovsk Region's steppe zone revealed similarities and differences in the morphology of leaf blades, leaf surface ultrastructure, and silicon localization in both forests and ravine slopes, based on the intensity of light the trees received. All four oak trees had identical leaf blade morphology. The leaf blades of the first two trees, located on the forest edge and shaded by other trees (trees No. 1 and No. 2), were significantly larger than those of trees No. 3 and No. 4 growing without shade on ravines. The leaf, being the most adaptable organ to environmental changes (Nevo, et al., 2000), shows the effects of environmental factors more clearly than stems and roots. Smaller leaf sizes can result in reduced water loss, especially from the adaxial surface. This has been observed in the leaves of two-year-old saplings of Quercus petraea and Q. robur, as reported by Dupouey and Dreyer [11], and in Olea europaea trees growing in environments with high air temperatures and low water supplies, as found by Bacelar, et al., [12]. Plants typically respond to shade by producing larger leaves with a lower mass per unit area, allowing for more efficient light capture per unit mass, as noted by Niinemets and Sack [13].

It is well-established that trees growing in sunnier areas produce smaller leaves with greater mechanical strength [14]. Additionally, these leaves have thicker cuticles and epicuticular wax layers. This phenomenon is also observed in the leaves of succulent and mesophytic plants, and also in plants grown under drought [15,16]. The unshaded leaves of plants that grow in direct sunlight are characterized by an increase in vessel and stomata density compared to shaded leaves [17,18]. Granier and Tardieu determined that the size of unshaded leaves is significantly affected by light intensity, which can impede cell division and elongation. This phenomenon can be attributed to shading as a prevailing

abiotic stressor, given its occurrence as a result of light obstruction by neighboring plants.

Our study found revealed differences in leaf structure between trees No. 1 and No. 2 grown under low light and shade, and trees No. 3 and No. 4 grown under high sun intensity. Specifically, we observed a reduced density of stomata and trichomes on the lower surface of shaded leaves compared to unshaded leaves. Karabourniotis and Bornman [17] also reported similar changes in stomata density when studing the impact of UV light on the morphology of oak and olive leaves. Previous studies have shown that a lack of light (80% shade) can disrupt the water balance in young oaks, specifically Q. velutina, leading to decreased transpiration activity, alterations in leaf water content, and an increase in water deficit [19]. Our study also found a direct correlation between the amount of solar radiation received and the structure of the stomatal apparatus in the leaves of Q. robur's petiole, as evidenced by the observed change in total stomata count. Changes in cuticle thickness and epicuticular wax on the abaxial surface of leaves have been documented for leaves of Q. rubra trees growing alone, not in groups with other trees [20], and for leaves of another oak species, Q. velutina, growing in direct sunlight [19]. Based on the literature and our research on the changes in stomatal density in oak leaves growing in southern Ukraine, we project that moderate drought will lead to optimized water balance and species conservation due to decreased stomatal density in shaded oaks.

Our research indicated that shaded oak trees (No. 1 and No. 2) have fewer simple non-glandular trichomes in their leaves compared to oak trees growing in non-shaded conditions (No. 3 and No. 4). The increase in trichome density in the unshaded oak trees (No. 3 and No. 4) is likely due to their role in protecting the leaves from environmental stressors. Simple elongated trichomes have been found in the leaves of various tree and grass species, including Q. laevis, red oak (Q. rubra), and black walnut (Juglans nigra) [21-26]. The increase in trichome density in unshaded oaks is thought to be related to their function as a barrier against UV radiation, increased transpiration, and pathogens [26]. These structures are crucial for the development of organs and are supported by phenolic compounds, specifically flavonoids. The formation of trichomes and the accumulation of phenolic compounds are linked at the molecular level. As non-glandular trichomes develop, they show significant morphological similarities to glandular trichomes. As they continue to grow and the secondary wall thickens, phenolic substances are moved to the cell walls of the trichomes [23,24].

Trichomes act as optical filters, protecting sensitive tissues from UV radiation by screening out harmful wavelengths through the scattered deposition of phenolics in the cell walls. The increased light reflectance on the surface provides protection against strong visible radiation [18,27]. Our research, in conjunction with the aforementioned publications, lead us to conclude that the leaf trichomes of oaks No. 3 and No. 4 protect the epidermis from high solar irradiation and reduce the intensity of cuticular transpiration.

We observed that the intensity of illumination did not

affect the presence of wax inclusions on the cell walls of the epidermis, the closing cells of stomata, and the base of trichomes on the adaxial and abaxial surfaces of leaves from four *Q. robur* trees in Ukraine's steppe zone. Wax can exist in cells in two forms: bound to the cuticle or free, creating crystals of different shapes on the cell surface [28]. The wax serves as a crucial barrier against unregulated water loss in leaves, has the capability to absorb and/or reflect UV radiation, and suppresses cuticular transpiration [4]. The presence of waxes has been noted in the leaves of different tree species [21,29]. The simultaneous presence of crystalline, liquid, and amorphous wax phases could be distinctive characteristics of various organs of numerous plant species [30,31].

The permeability of the amorphous phase is determined by the degree of crystallinity of the wax and the spatial structure of the crystals, which affects the effectiveness of the diffusion barrier. The study concludes that epicuticular waxes remain on the leaf surface and limit access to the pores in the cuticle. Based on the data regarding the role of wax on leaf surfaces and our experimentation results on the existence of wax on the anticlinal walls of the upper epidermis and on all types of cells of the abaxial epidermis of leaves from four *Q. robur* trees, we can deduce the following hypotheses:

- 1. Crystalline wax is a structural hallmark of oak leaves, regardless of the light intensity.
- The wax in the cells of the oak tree's lower epidermis regulates transpiration and optimizes the leaf blade's water balance.

Silicon in plant cells functions as a biological lens, helping incident infrared light penetrate efficiently inside cells and leaves when combined with carbohydrates, proteins, or lipids in the cell walls [32,33], These properties can facilitate efficient heating of plants as absorbed far-infrared light is converted into heat [34,35]. Silicon inclusions (8-12 μm in size) in the epidermis effectively cool leaves via highly efficient thermal radiation in the mid-infrared range, according to Wang, et al., [5]. Stomatal transpiration also cools leaves. Reduction of transpiration in plants can be achieved by depositing silica structures in the leaf epidermis. This approach may be practical and environmentally friendly for improving plant resistance to high temperatures. The results indicate that plants infused with bio-silicon and subjected to temperature stress employ an uncomplicated physical strategy to defend against heat stress. Besides, Turkish Researchers have shown that exogenous application of silicon mitigates the harmful effects of salinity on plants, improving gas exchange and plant productivity by strengthening the enzymatic and nonenzymatic (proline and glycine betaine) antioxidant defence system [36]; and also under conditions of water deficit, silicon had a positive effect on growth and photosynthesis intensity, as shown in wheat seedlings [37].

Silicon is capable of absorbing light fluxes ranging from infrared to ultraviolet. In plants, the refractive index of silicon structures is approximately equal to the wavelength of visible light. As a result, not only do such structures absorb light, they also reflect it in the region of wavelengths referred to as the photonic band gap [38,39]. This optical phenomenon is

due to the slowing down of light's group speed at the edges of the photon zone. In this scenario, the interaction between light and materials is intensified. Periodic silicon structures facilitate the enhancement of light reflection and absorption, while higher plants possess characteristic structures that sense infrared or far-infrared radiation. Pedrotti and Leno [40] indicate that the radius of curvature and size of an object are significant parameters for light reflection. Sunbeams can remain unaltered in direction based on the thickness and curvature of the lens. The periclinal walls of the upper epidermis of oak leaves, which we examined, exhibited diverse shapes, either convex or concave depending on the degree of illumination. We were able to identify them as a convex lens (oaks No. 1, 3, and 4), a concave lens (oaks No. 2), or a cylindrical lens, which correspond to the anticlinal walls of the epidermis of all examined samples. The question of UV ray transmission, absorption, and reflection intensity through cell walls acting as lenses remains unanswered and requires further study by biophysicists.

Researchers recently discovered silicon-rich trichomes on both the upper and lower leaf surfaces of the Aphananthe aspera (Muku tree) in Osaka, Japan [35]. The team used infrared spectroscopy to analyze the trichomes and found that they play a significant role in absorbing far-infrared light due to specific chemical bonds in organic materials and silica. Further research in southern Ukraine confirmed the presence of silicon inclusions in the upper and lower leaf epidermal cells of all oak trees surveyed. The magnitude of the silicon profile varied depending on the type of epidermis and cell. Observations showed that oak trees grown in direct sunlight had greater silicon fluorescence in the cell walls of trichomes, stomata, and upper and lower epidermal cells. This led to the conclusion that increasing silicon content in these areas enhances sunlight absorption and reflection, optimizing photon content for improved photosynthesis and thermal stability.

The study of silicon inclusions in oak leaves has potential applications in botany, medicine, pharmacology, and agriculture. Plants with high silicon content, such as oak trees, have been found to be beneficial for bone tissue restoration in medicine [1,41]. Additionally, the use of oak leaves as fertilizer has shown positive results in agriculture, particularly in improving plant health under water stress conditions. The application of oak leaves as fertilizer in agriculture yields positive results by optimizing the Researchers found that adding oak leaf powder and biofertilizer to soil improved the growth and biochemical composition of tomato leaves of several genotypes under water stress conditions [42]. In conclusion, this study highlights the potential benefits of oak leaves for mitigating water stress and improving plant life, making them promising for practical applications in agriculture and medicine.

Conclusions

The study found differences in the leaf epidermis of *Q. robur* trees grown in shade versus direct sunlight in the southern steppes of Ukraine. Trees grown in direct sunlight had smaller leaves, more stomata and trichomes, and a

bulge in the periclinal cell walls on the adaxial surface. These features help reflect sunlight from the upper surface of sunlit oak leaves compared to shaded leaves. These structural features show that oak leaves have the ability to adapt to high solar irradiation. The presence of silicon inclusions in oak leaf epidermal cells indicates that intense solar radiation increases the silicon content in the leaf epidermis. Oak leaves containing silicon can be used in pharmacology and industry.

Acknowledgements

This study was financially supported by the Department of General Biology of the National Academy of Sciences of Ukraine, under the budget topic "Phenotypic Variability of Structural and Physiological Traits of Common Oak (Quercus Robur L.) in Conditions of Aridization of the Ukrainian Climate", 6541230 (fundamental research) (KITKB 6541230).

Conflict of Interest

The author declares no conflicts of interest related to this research, authorship, or publication.

Thanks

Thank you Drs. Shevchenko G. and Baranovsky B. assisted with collecting samples for the study.

Auto Contribution

Dr. Nedukha O. independently conducted experiments, fixed and photographed samples, examined those using electron and laser confocal microscopes, described the results, and wrote a manuscript of the article.

References

- 1. Taib M, Rezzak Y, Bouyazza L, et al. (2020) Medicinal uses, phytochemistry, and pharmacological activities of Quercus species. Evid Based Complement Alternat Med 20: 1-20.
- 2. Novak A (2005) Modern state of the oak planting in a techniques zone of JSC "Mykolayivcement". Scientific Bulletin: Collection of scientific and technical papers. Lviv: UkrDLTU. Issue 15: 53-57.
- 3. Broome A, Mitchel R, Ray D, et al. (2021) Ecological implications of oak decline in Great Britain. Forest Res 1-12.
- Riederer M, Schreiber L (2001) Protecting against water loss: Analysis of the barrier roperties of plant cuticles. J Exp Bot 52: 2023-2032.
- 5. Wang Lijun, Nie Q, Li M, et al. (2005) Biosilicified structures for cooling plant leaves: A mechanism of highly efficient midinfrared thermal emission. Appl Phys Lett 87: 1-3.
- Mirshafieyan S, Guo J (2014) Silicon colors: spectral selective perfect light absorption in single layer silicon films on aluminum surface and its thermal tenability. Optics Express 22: 31545-31554.
- 7. Pandey SK, Singh H (2011) A Simple, Cost-Effective Method for Leaf Area Estimation. J Botany 2011.
- Vasic PS, Dubak DV (2012) Anatomical analysis of red Jiniper leaf (Jiniperus oxycedrus) taken from Kopaonik Moutain, Serbia. Turk J Botany 36: 473-479.
- 9. Talbot M, White R (2013) Cell surface and cell outline imaging in plant tissues using the backscattered electron detector in a

- variable pressure scanning electron micro-scope. Plant Methods 9: 1-16.
- 10. Dabney C, Ostergaard J, Watkins E, et al. (2016) A novel method to characterize silica bodies in grasses. Plant Methods 12: 3-10.
- 11. Ponton S, Dupouey JL, Dreyer E (2004) Leaf morphology as species indicator in seedlings of Quercus robur L. and Q. petraea (Matt.) Liebl.: modulation by irradiance and growth flush. Ann For Sci 61: 73-80.
- 12. Bacelar E, Correia C, Mountinho J, et al. (2004) Sclerophylly and leaf anatomical traits of five field-grown olive cultivars growing under drought conditions. Tree Physiol 24: 233-239.
- Niinemets Ü, Sack L (2006) Structural determinants of leaf light harvesting capacity and photosynthetic potentials. In: K Esser, U Lüttge, W Beyschlag, et al., Progress in Botany, Book Series. 67: 385-419.
- Onoda Y, Schieving F, Anten N (2008) Effects of light and nutrient availability on leaf mechanical properties of Plantago major: A conceptual approach. Ann Bot 101: 727-736.
- 15. Richardson AD, Berlyn GP (2002) Change in foliar spectral reflectance and chlorophyll fluorescence of four temperate species following branch cutting. Tree Physiology 22: 499-506.
- 16. Nevo E, Pavlek T, Beharay A, et al. (2013) Droughtand light anatomical adaptive leaf strategies in three woody species caused by microclimatic selection at Evolution Canyon, Israel. Isr J Plant Sci 48: 33-46.
- 17. Karabourniotis G, Bornman J (1999) Penetration of UV-A, UV-B and blue light through the leaf trichome layers of two xeromorphicplants, olive and oak, measured by optical fibre microprobes. Physiologia Plantarum 105: 655-661.
- 18. Karabourniotis G, Liakopoulos G, Nikolopoulos D, et al. (2020) Protective and defensive roles of non-glandular trichomes against multiple stresses: Structure-function coordination. J Fores Res 31: 1-12.
- 19. Osborn J, Taylor T (1990) Morphological and ultrastructural studies of plant cuticular membranes. I. Sun and shade leaves of quercus velutina (Fagaceae). Botanical Gazette 151: 465-476.
- 20. Kryvoruchko A, Bessonova V (2018) Anatomical leaves characteristics of Quercus rubra L. and Quercus robur L. and stand density. Ukr J Ecol 8: 64-71.
- Prasad R, Gülz R-G (1990) Surface structure and chemical composition of leaf waxes from Quercus robur L., Acer pseudoplatanus L. and Juglans regia L. Zeitschrift fur Naturforschung 45: 813-817.
- 22. Wagner G, Wang E, Shepherd R (2004) New approaches for studying and exploiting an old protuberance, the plant trichome. Ann Bot 93: 3-11.
- 23. Chen Z, Ren H, Wen J (2007) Vitaceae. In: Wu CY, Hong DY, Raven PH, Flora of China, Vol. 12. Science Press, Beijing, and Missouri Botanical Garden Press, St. Louis, 173-222.
- 24. LoPresti E (2015) Chemicals on plant surfaces as a heretofore unrecognized, but ecologically informative, class for investigations into plant defence. Biol Rev Camb Philos Soc 91: 1102-1117.
- 25. Oksanen E (2018) Trichomes form an important first line of defence against adverse environment-New evidence for ozone stress mitigation. Plant Cell Environ 41: 1497-1499.
- 26. Wang X, Shen Ch, Meng P, et al. (2021) Analysis and review of trichomes in plants. BMC Plant Biol 21: 70.

- 27. Skaltsa E, Verykokidou E, Harvala C, et al. (1994) UV-B protective potential and flavonoid content of leaf hairs of Quercus ilex. Phytochemistry 37: 987-990.
- 28. Kerstiens G (1996) Cuticular water permeability and its physiological significance. J Exp Bot 47: 1813-1832.
- 29. Prasad R, Moller E, Gülz R-G (1990) Epicuticular waxes from leaves of Quercus robur. Phytochem Photobiol 29: 2101-2103.
- 30. Reynhardt E, Riederer M (1994) Structures and molecular dynamics of plant waxes. II. cuticular waxes from leaves of Fagus sylvatica L. and Hordeum vulgare L. Eur Biophys J 23: 59-70.
- 31. Müller C, Riedere M (2005) Plant surface properties in chemical ecology. J Chem Ecol 31: 2621-2651.
- 32. Guerriero G, Hausman J, Legay S (2016) Silicon and the plant extracellular matrix. Front Plant Sci 7: 463.
- 33. Grašič M, Vogel-Mikuš K, Gaberščik A, et al. (2020) Do soil and leaf silicon content affect leaf functional traits in Deshampsia caespitosa from different habitats? Biologia Plantarum 64: 234-243.
- 34. Ma FJ, Yamaji N, Mitani-Ueno N (2011) Transport of silicon from roots to panicles in plants. Proc Jpn Ser B Phys Biol Sci 87: 377-385.
- 35. Takeda H, Ito F, Yamanaka S, et al. (2013) Roles of trichomes with silica particles on the surface of leaves in Aphananthe aspera. AIP Advances 3: 1-5.

- 36. Adnan SM, Mukhtar BR, Aslam PM, et al. (2015) Foliar spray of phyto-extracts supplemented with silicon: An efficacious strategy to alleviate the salinity-induced deleterious effects in pea (Pisum sativum L.). Turk J Botany 39: 408-419.
- 37. Maghsoudi K, Emam Y, Ashraf M (2015) Influence of foliar application of silicon on chlorophyll fluorescence, photosynthetic pigments, and growth in water-stressed wheat cultivars differing in drought tolerance. Turk J Botany 39: 625-634.
- Mckenzie D, Large M (1998) Multilayer reflectors in animals using green and gold beetles as contrasting examples. J Exp Bot 201: 1307-1313.
- 39. Yahaya N, Yamada N, Kotaki Y, et al. (2013) Characterization of light absorption in thin-film silicon with periodic nanohole arrays. Optics Express 21: 5924-5930.
- 40. Pedrotti F, Leno S, Leno M (2007) Introduction to Optics. (3rd edn), Pearson Prentice Hall, 1-221.
- 41. Kolesnikov MP, Gins VK (2001) Forms of silicon in medicinal plants. Appl Biochem Microbiol 37: 524-527.
- 42. Abdul-Razzak Tahir N, Rasul KS, Lateef DD, et al. (2022) Effects of oak leaf extract, biofertilizer, and soil containing oak leaf powder on tomato growth and biochemical characteristics under water stress conditions. Agriculture 12: 2082.

DOI: 10.36959/771/577

Copyright: © 2024 Nedukha O. This is an open-access article distributed under the terms of the Creative Commons Attribution License, which permits unrestricted use, distribution, and reproduction in any medium, provided the original author and source are credited.

